

Electronic Supplementary Information

Impact of nanosizing a host matrix based on a metal-organic framework on solid-state fluorescence emission and energy transfer

Hikaru Sakamoto,[†] Akitaka Ito,[†] and Masataka Ohtani,^{†,*}

[†]School of Environmental Science and Engineering, Kochi University of Technology

185 Miyanokuchi, Tosayamada, Kami, Kochi 782-8502, Japan

E-mail: ohtani.masataka@kochi-tech.ac.jp (M.O.)

Supporting Figures

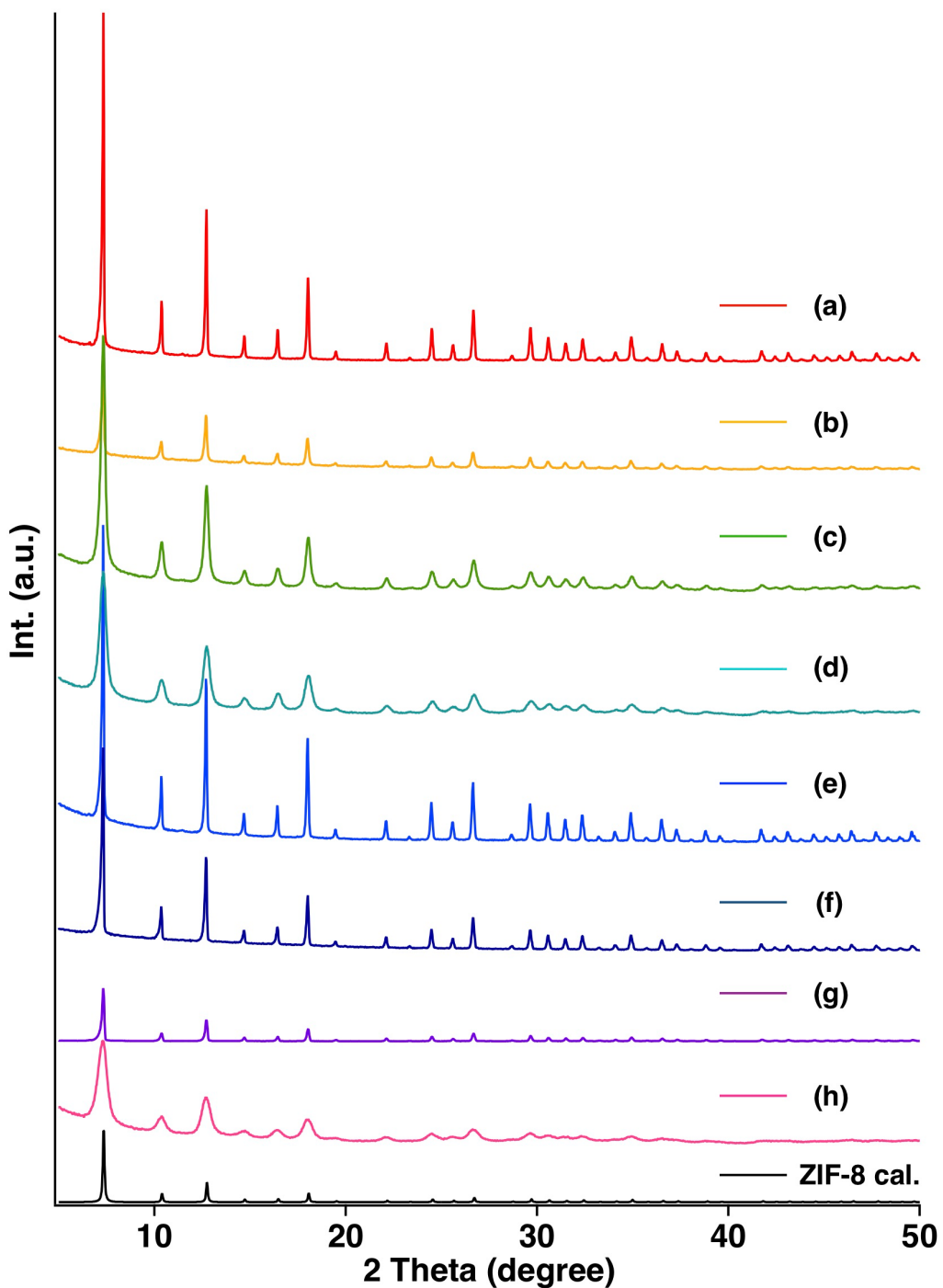


Figure S1. PXRD patterns of ZIF-8 synthesized with different conditions: (a) MeOH, (b) EtOH, (c) MeCN, (d) benzonitrile, (e) EG, (f) MeOH (4 °C), (g) MeOH (the precursor zinc solution without 1-MIm), and (h) MeOH with adding triethylamine (1 eq. amount based on 2-MIm), and calculated ZIF-8 reference (CCDC: 864309).

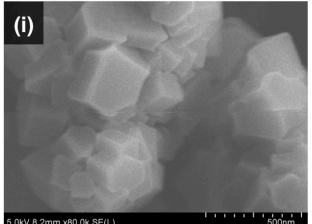
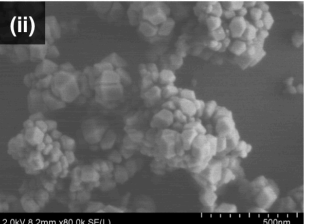
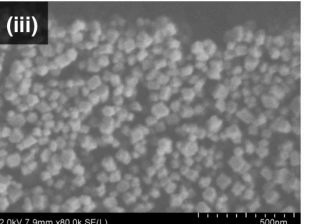
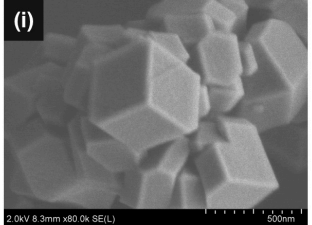
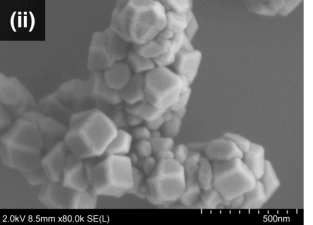
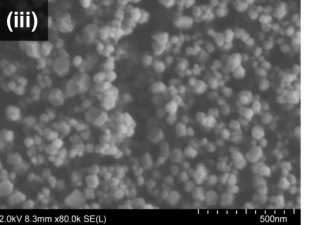
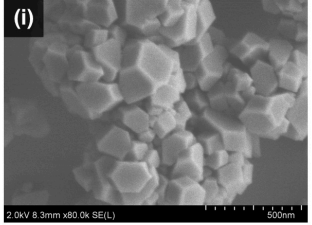
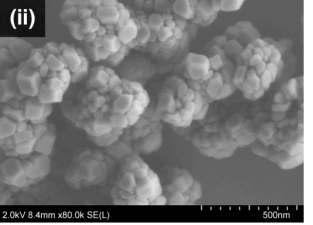
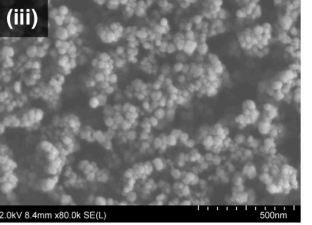
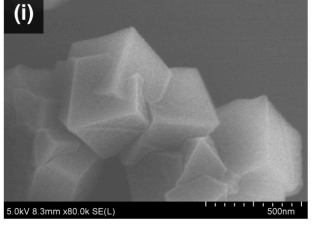
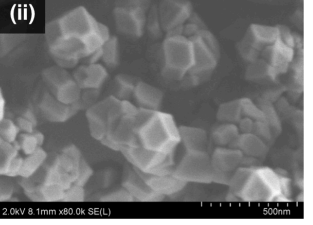
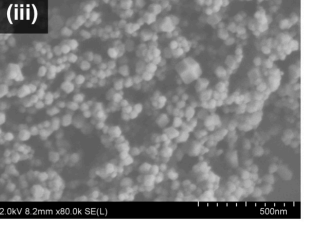
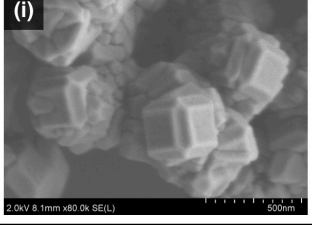
Solvent	25 °C	50 °C	Boiling point
a) Ethanol	(i)  5.0kV 8.2mm x80.0k SE(L) 500nm	(ii)  2.0kV 8.2mm x80.0k SE(L) 500nm	(iii)  2.0kV 7.9mm x80.0k SE(L) 500nm
b) 1-Propanol	(i)  2.0kV 8.3mm x80.0k SE(L) 500nm	(ii)  2.0kV 8.5mm x80.0k SE(L) 500nm	(iii)  2.0kV 8.3mm x80.0k SE(L) 500nm
c) 2-Propanol	(i)  2.0kV 8.3mm x80.0k SE(L) 500nm	(ii)  2.0kV 8.4mm x80.0k SE(L) 500nm	(iii)  2.0kV 8.4mm x80.0k SE(L) 500nm
d) 1-Butanol	(i)  5.0kV 8.3mm x80.0k SE(L) 500nm	(ii)  2.0kV 8.1mm x80.0k SE(L) 500nm	(iii)  2.0kV 8.2mm x80.0k SE(L) 500nm
e) 2-Butanol	(i)  2.0kV 8.1mm x80.0k SE(L) 500nm		

Figure S2. SEM images of ZIF-8 synthesized with the different solvent: (a) EtOH, (b) 1-PrOH, (c) 2-PrOH, (d) 1-BuOH, and (e) 2-BuOH and different reaction temperatures (room temperature, 50 °C, and near the boiling point of each solvent) in each solvent.

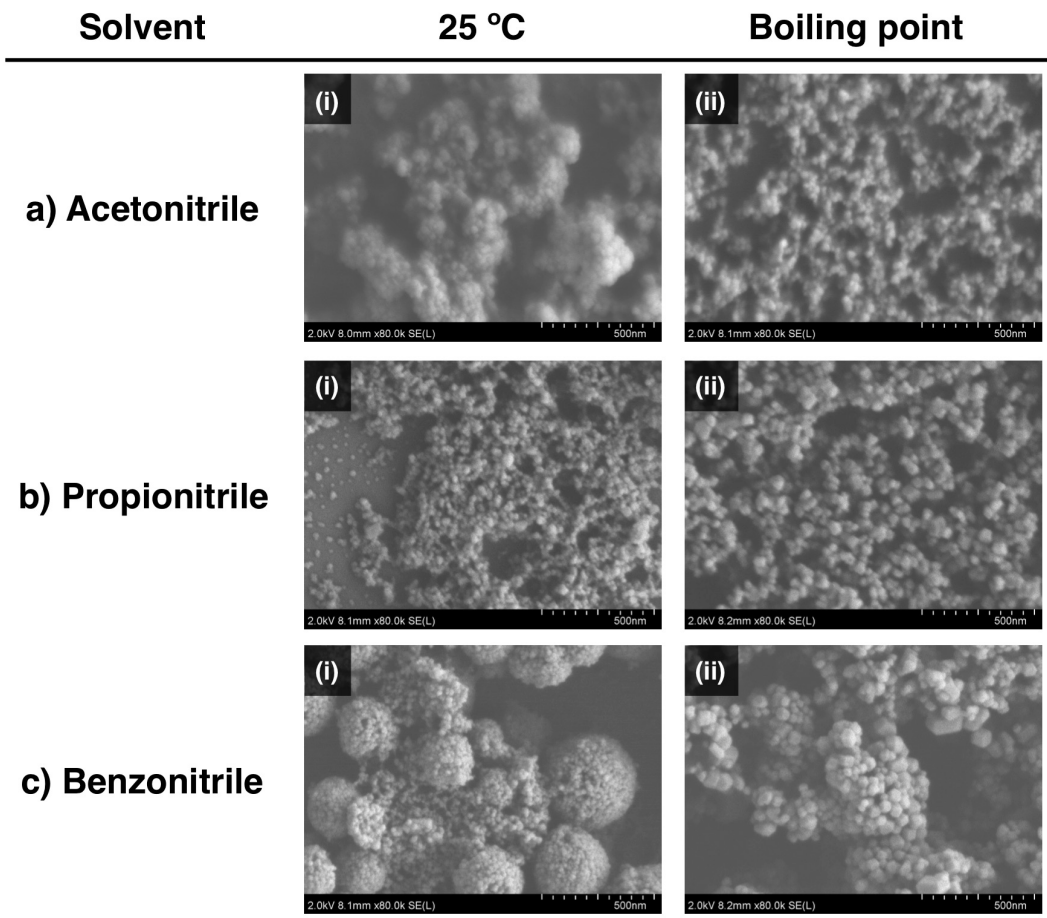


Figure S3. SEM images of ZIF-8 synthesized with (a) MeCN, (b) propionitrile, (c) benzonitrile, and different reaction temperatures (room temperature, 50 °C, and near the boiling point of each solvent) in each solvent.

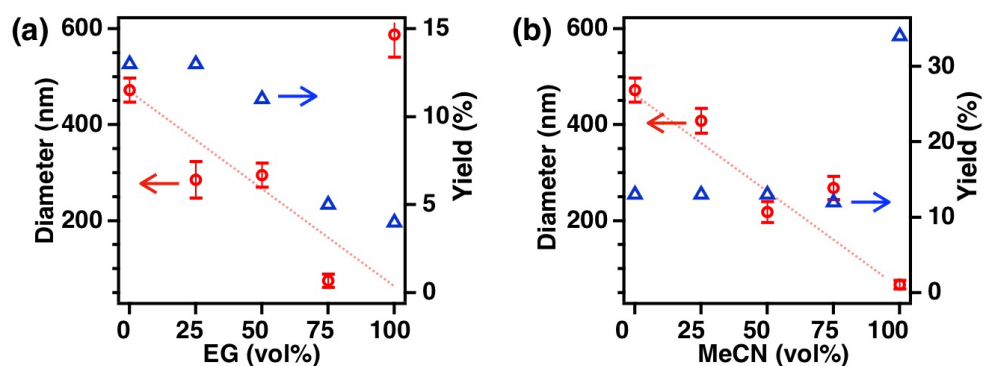


Figure S4. (a) Crystal size distribution and/or product yield versus the volume ratio of EG in MeOH, and (b) particle size distribution and/or product yield versus the volume ratio of MeCN in MeOH.

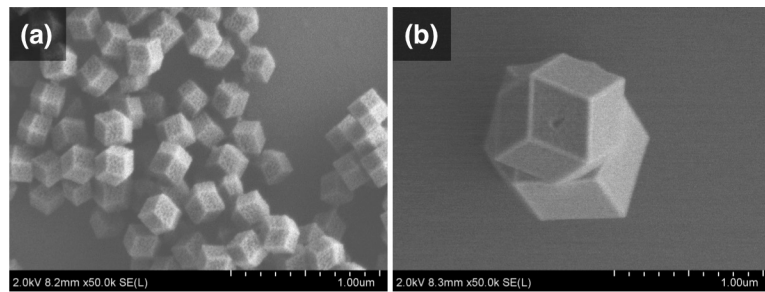


Figure S5. (a) SEM images of ZIF-8 synthesized in MeOH at 50 °C (a) and (b) 4 °C.

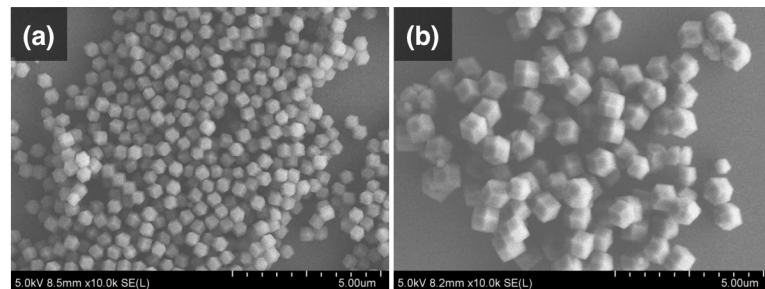


Figure S6. SEM images of ZIF-8 synthesized in MeOH at room temperature: (a) addition of 1-MIm to the precursor zinc solution, and (b) without 1-MIm.

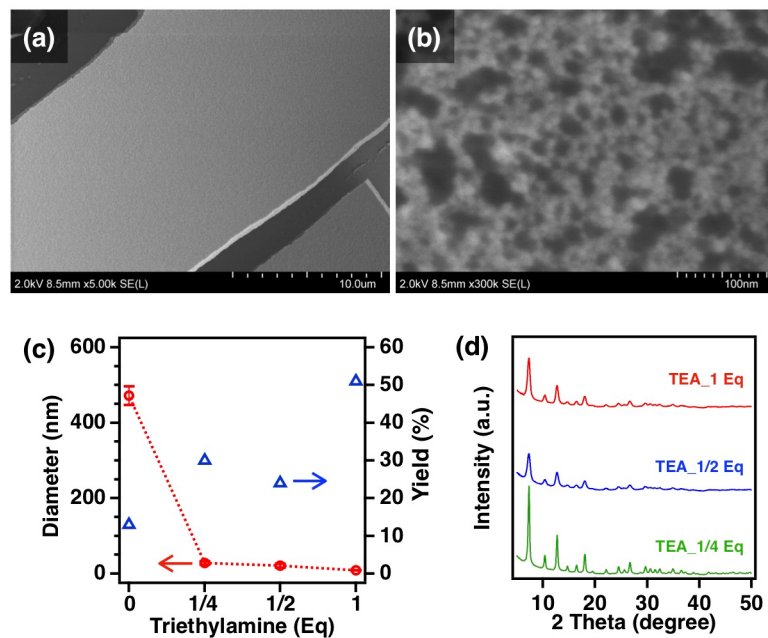


Figure S7. SEM images of ZIF-8: each magnification is (a) x5k, (b) x300k, and crystal size distribution and/or product yield versus the equivalent amount of triethylamine (TEA) to Zn-ion content. (d) XRD patterns of ZIF-8 synthesized with different amount of TEA: (red) 1 eq., (blue) 0.5 eq., and (green) 0.25 eq..

Table S1. Crystal size of ZIF-8 synthesized with different conditions

solvent	Temperature (°C)	TEA (ep)	Diameter (nm)	Yield (%)
Methanol	3–4	—	1041 ± 110	11
Ethylene glycol	r.t.	—	588 ± 47	5
Methanol	r.t.	—	472 ± 25	13
Methanol	50	—	256 ± 16	15
Ethanol	70	—	72 ± 15	12
Acetonitrile	r.t.	—	55 ± 8	34
Methanol	r.t.	1/4	28 ± 4	30
Methanol	r.t.	1/2	21 ± 5	23
Acetonitrile	r.t.	1	17 ± 3	70
Methanol	r.t.	1	9	51

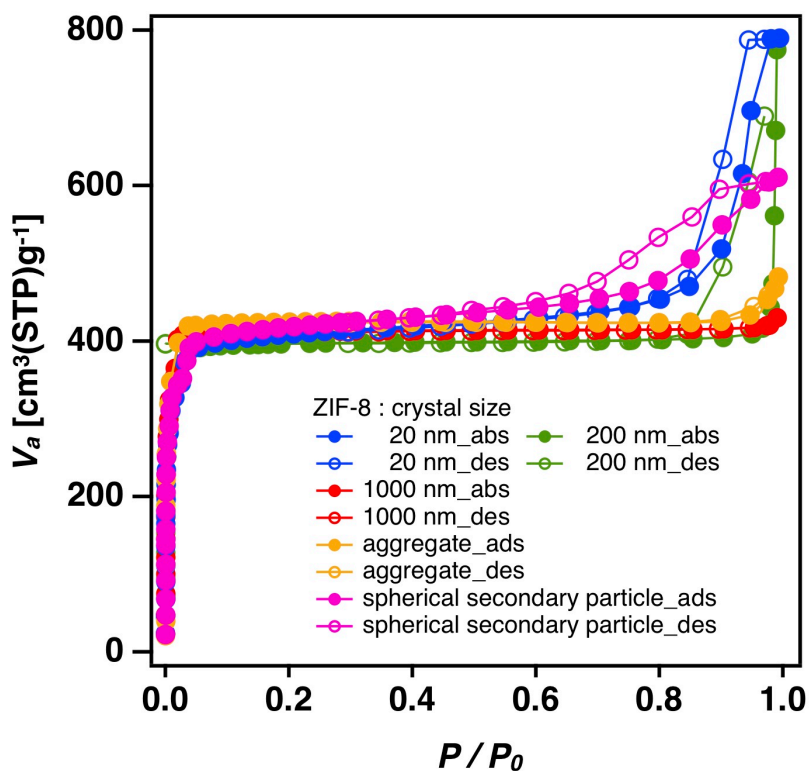
**Figure S8.** Nitrogen adsorption (solid symbol) and desorption (open symbol) isotherms of ZIF-8: crystal size_(blue) ca. 20 nm, (green) ca. 200 nm, (red) ca. 1000 nm, (yellow) 500-nm-sized aggregate (Figure S2a_r.t.) and (purple) spherical secondary nanoparticle (Figure S3c-i).

Table S2. Nitrogen gas adsorption/desorption analysis of ZIF-8 crystals

crystal size (nm)	specific surface area, S_{BET} (m^2/g)	pore volume (cm^3/g)	pore diameter (nm)
20	1600	1.2	3.0
200	1600	1.2	3.0
1000	1640	0.7	1.6
aggregate	1740	0.7	1.7
spherical secondary nanoparticle	1630	0.9	2.3

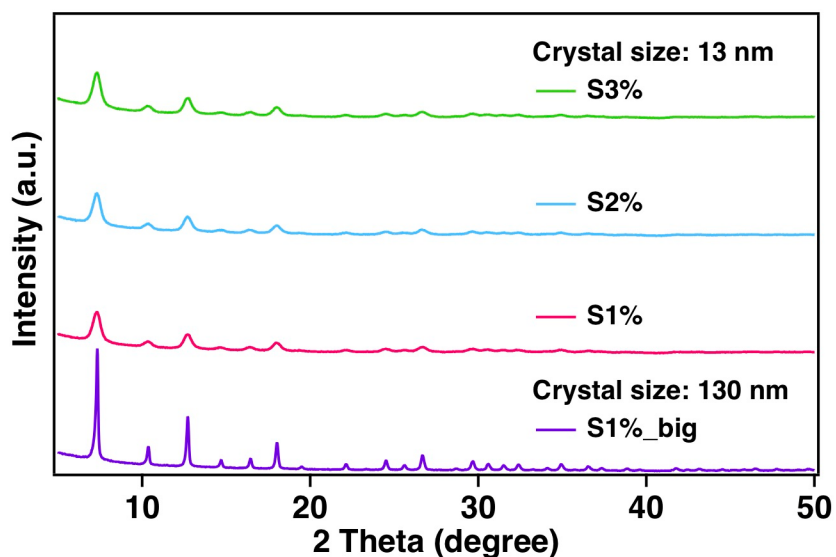


Figure S9. XRD patterns of ANS@ZIF-8 with different crystal sizes and amounts of ANS in ZIF-8: (green) 13 nm_S3%, (blue) 13 nm_S2%, (pink) 13 nm_S1%, (violet) 130 nm_S1%. The content of sulfur due to ANS was determined with atomic% (at%) relative to Zn-ion in ZIF-8 by STEM-EDX analysis.

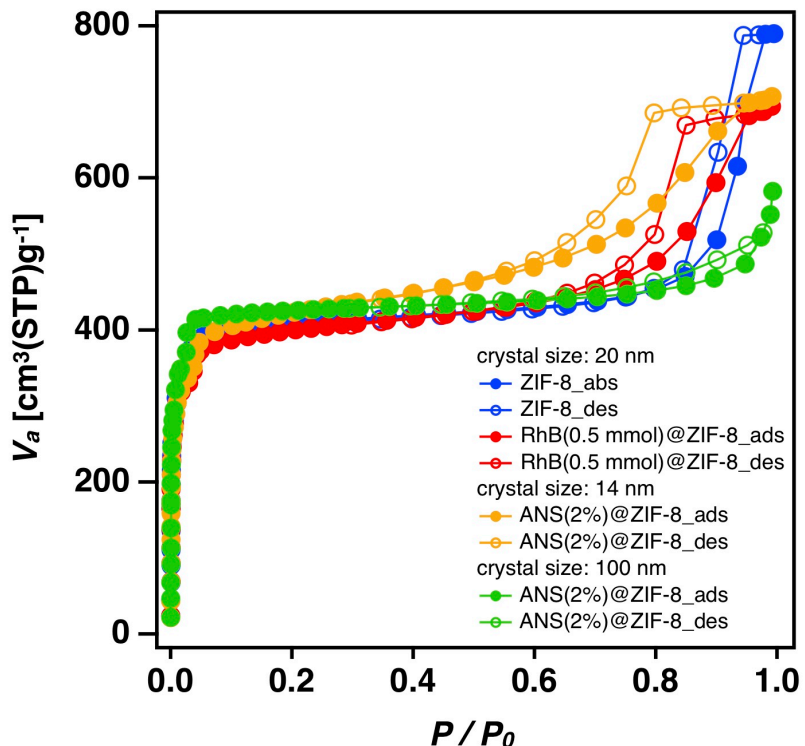


Figure S10. Nitrogen adsorption (solid symbol) and desorption (open symbol) isotherms of Samples: (blue) 20 nm sized ZIF-8, (red) RhB(0.5 mmol)@ZIF-8, (yellow) 14 nm sized ANS(2%)@ZIF-8 and (green) 100 nm sized ANS(2%)@ZIF-8.

Table S3. Nitrogen gas adsorption/desorption analysis of Samples

sample	crystal size (nm)	specific surface area, S_{BET} (m ² /g)	pore volume (cm ³ /g)	pore diameter (nm)
nanoZIF-8	20	1600	1.2	3.0
RhB(0.5 mmol) @ZIF-8	20	1460	1.0	2.9
	14	1580	1.1	2.8
ANS(2%)@ZIF-8	100	1680	1.0	2.1

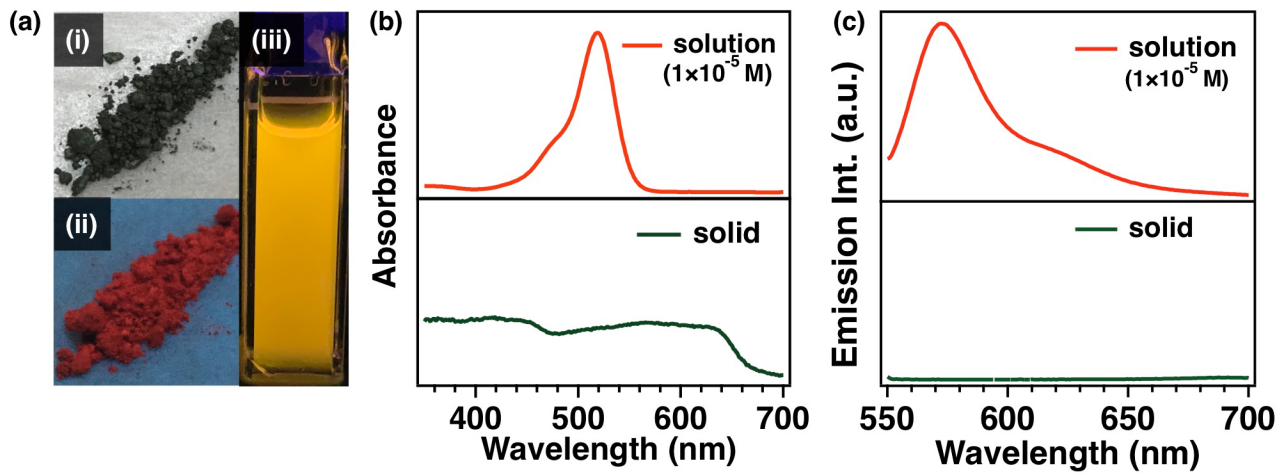


Figure S11. Photographs of solid-state RhB under visible light (a-i), under UV light (a-ii), RhB solution in MeCN ($10 \mu\text{mol/L}$) under UV light (a-iii). (b) UV-vis absorption spectra and (c) fluorescence spectra of (red) RhB in MeCN solution state and (green) RhB in solid state.

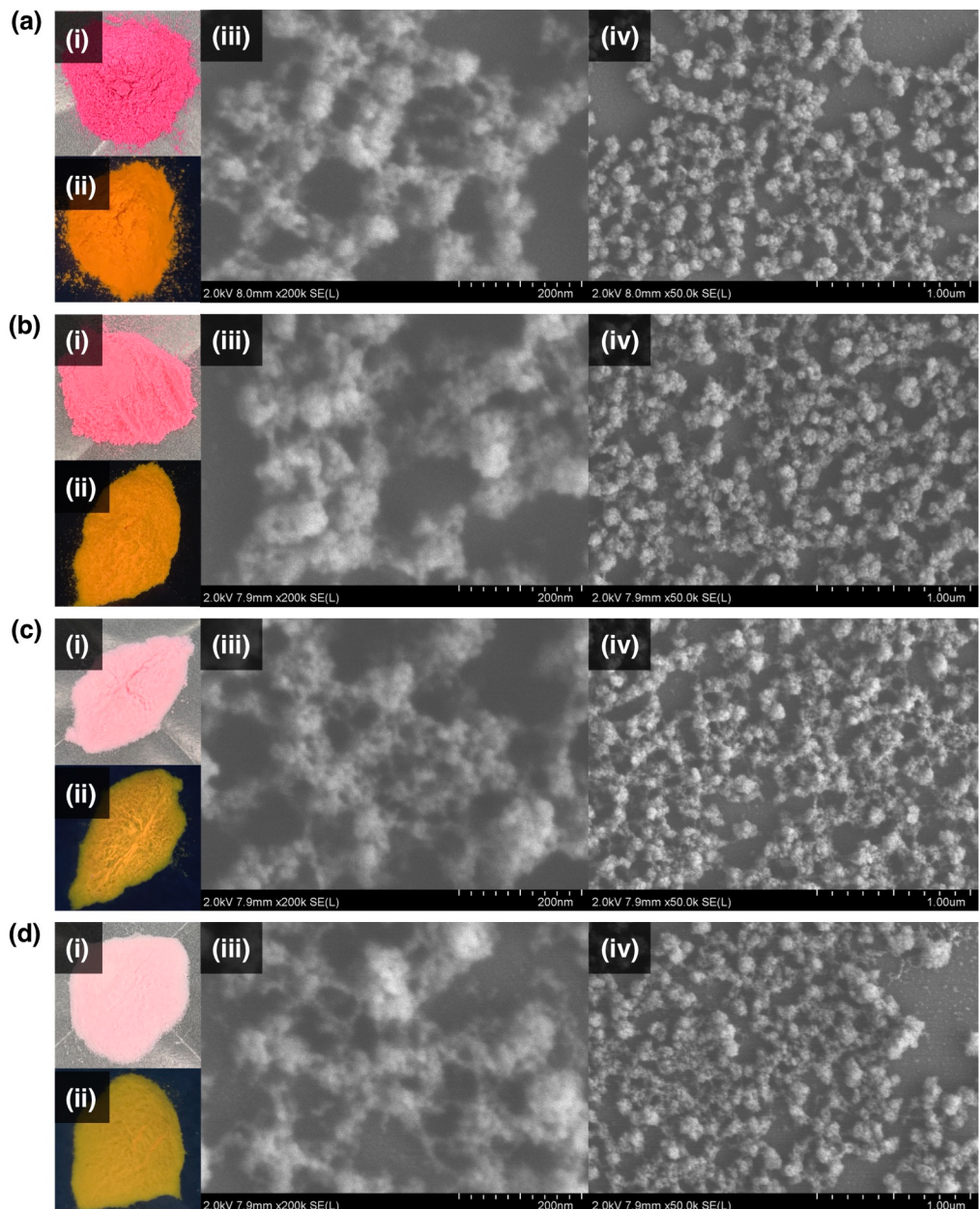


Figure S12. Photographs of 14 nm-sized RhB@ZIF-8 under visible light (i), under UV light (ii), and SEM images at x200k (iii) and x50k (iv) magnification: The initial concentrations of RhB are (a) 0.5 mmol, (b) 0.25 mmol, (c) 0.02 mmol, (d) 0.01 mmol, respectively.

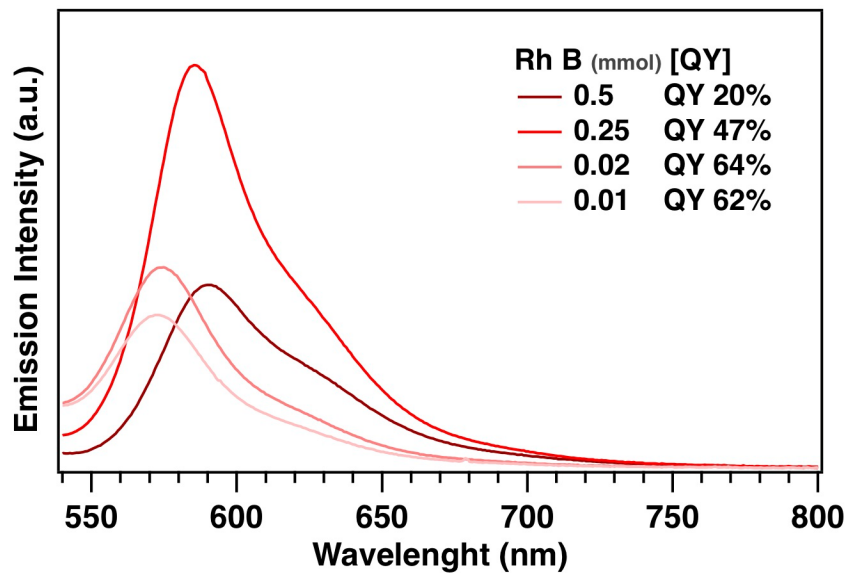


Figure S13. Solid-state fluorescence spectra of RhB@ZIF-8 with different encapsulation amounts of RhB: The initial concentration of RhB are (dark red) 0.5 mmol, (b) 0.25 mmol, (c) 0.02 mmol, (d) 0.01 mmol.

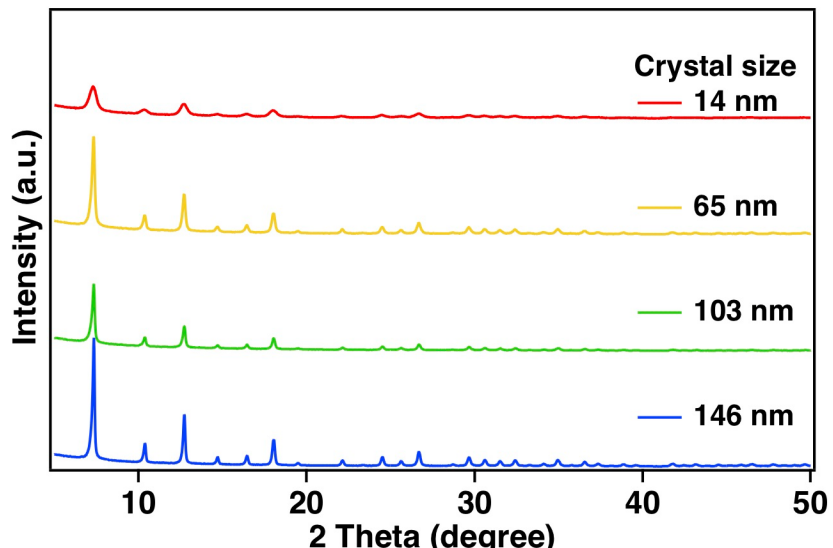


Figure S14. PXRD patterns of RhB(0.25 mmol)@ZIF-8 with different crystal sizes: Crystal size are (red) 14 nm, (yellow) 65 nm, (green) 103 nm, (blue) 146 nm, respectively.

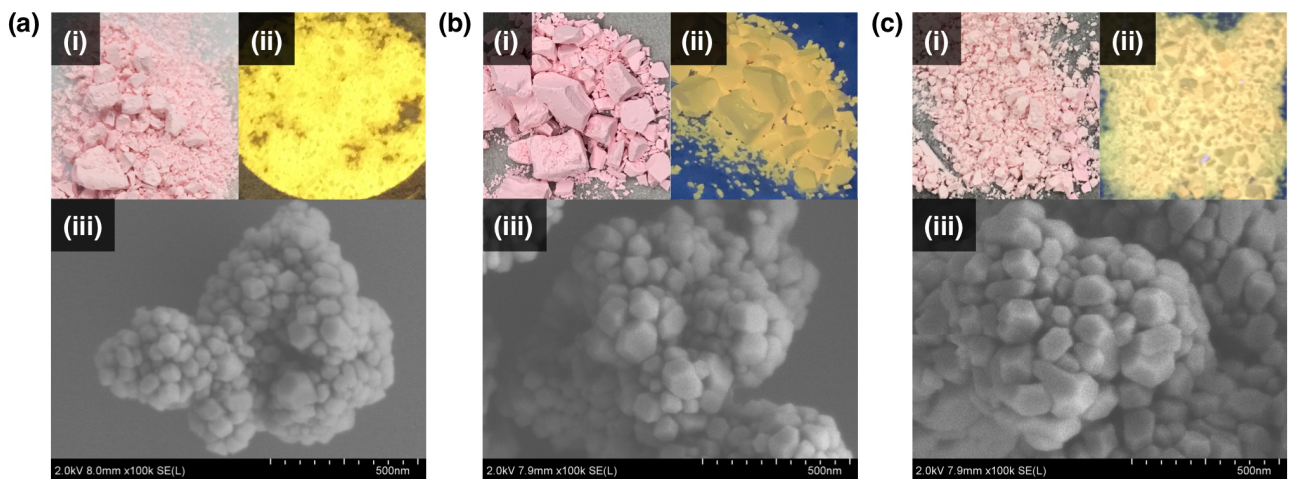


Figure S15. Photographs of RhB(0.25 mmol)@ZIF-8 with different crystal sizes under visible light (i), under UV light (ii), and SEM images (iii): Crystal size are (red) 14 nm, (yellow) 65 nm, (green) 103 nm, (blue) 146 nm.

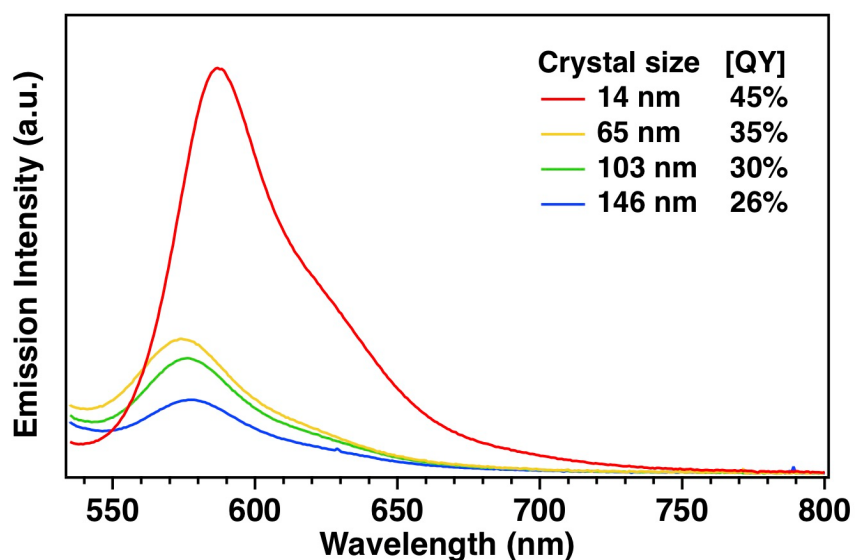


Figure S16. Solid-state fluorescence spectra of RhB(0.25 mmol)@ZIF-8 with different crystal sizes: Crystal size are (red) 14 nm, (yellow) 65 nm, (green) 103 nm, (blue) 146 nm.

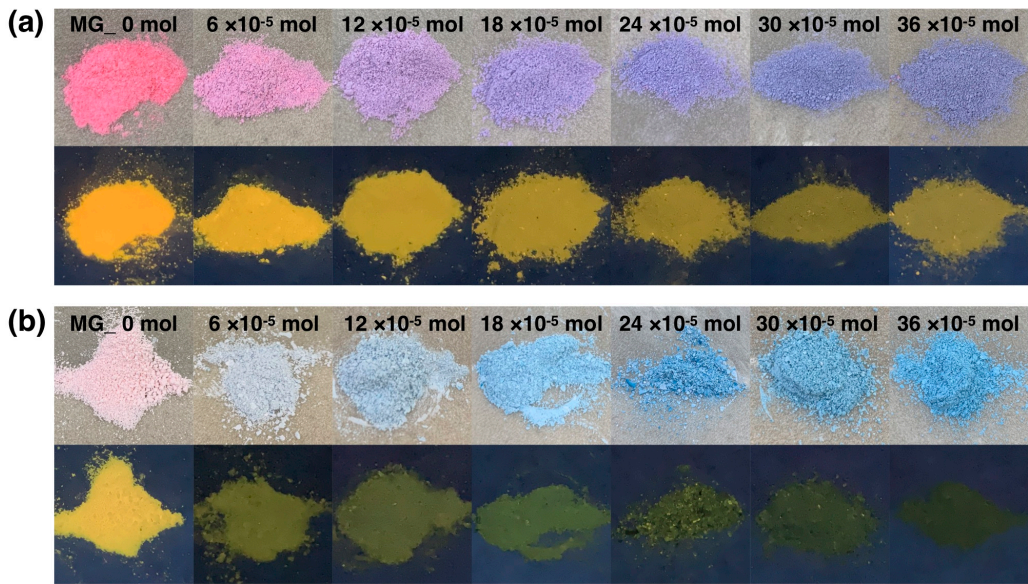


Figure S17. Photographs of (a) 16 nm-sized MG-RhB@ZIF-8 and (b) 75 nm-sized MG-RhB@ZIF-8.

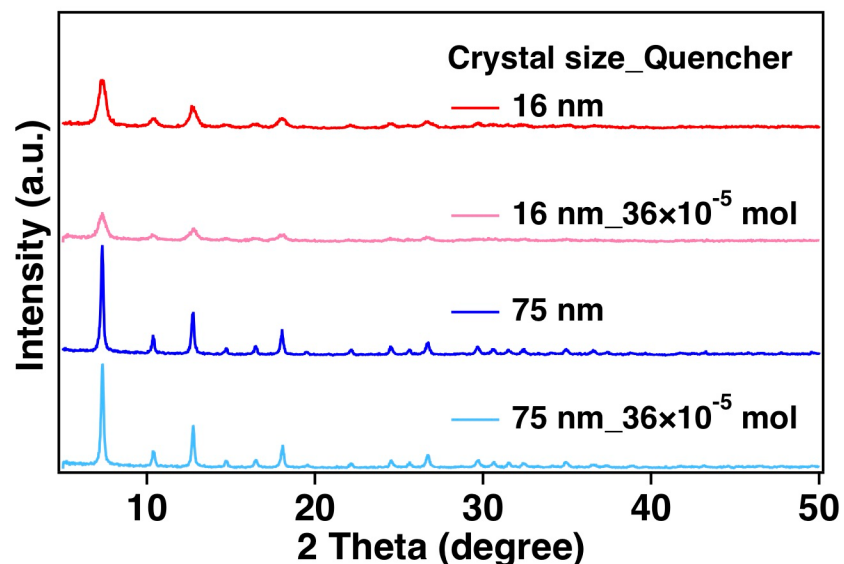


Figure S18. PXRD patterns of samples: (red) 16 nm-sized Rh B@ZIF-8 was obtained without quencher, (pink) Rh B@ZIF-8 with adsorbed MG (36×10^{-5} mol), (blue) 75 nm-sized Rh B@ZIF-8 was obtained without quencher, (light blue) Rh B@ZIF-8 with adsorbed MG (36×10^{-5} mol).

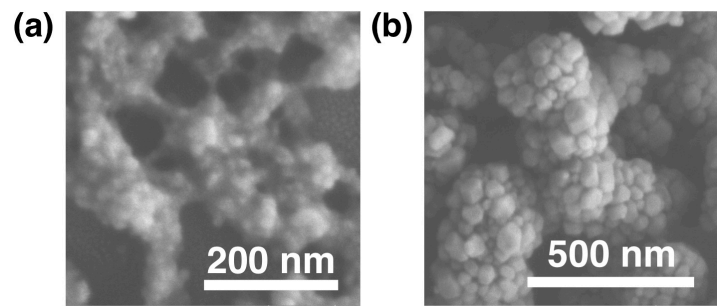


Figure S19. SEM images of (a) 16 nm-sized Rh B@ZIF-8 and (b) 75 nm-sized Rh B@ZIF-8.

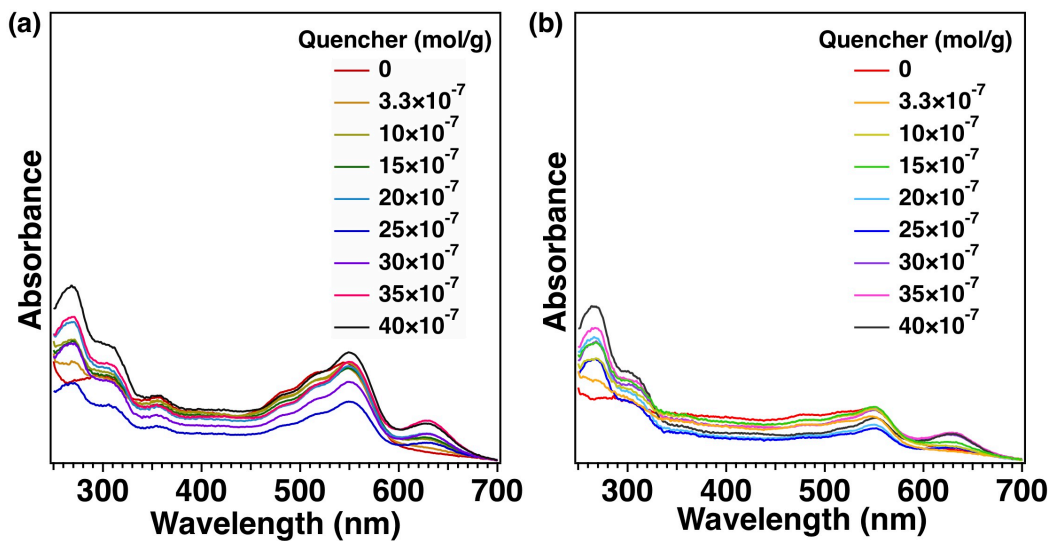


Figure S20. Solid-state UV-vis absorption spectra of (a) 16 nm-sized Rh B@ZIF-8 and (b) 75 nm-sized Rh B@ZIF-8.

Table S4. Quenching efficiency of RhB solution, 16 nm-sized RhB@ZIF-8 and 75 nm-sized RhB@ZIF-8.

Rh B solution		RhB@ZIF-8		
Quencher concentration (10^{-9} mol)	Quantum yield (%)	Quencher concentration (10^{-5} mol)	Nano crystal Quantum yield (%)	Sub-micro crystal Quantum yield (%)
0	32	0	50	38
2	21	1.5	34	29
4	15	3	29	22
6	11	6	23	16
8	9	9	14	8
10	8	12	10	7
12	7	18	11	3
16	6	24	8	2
20	5	30	6	1
24	4	36	6	0